The International Journal of Advanced Manufacturing Technology (2021) 115:2395–2402
https://doi.org/10.1007/s00170-021-07242-9

ORIGINAL ARTICLE

AZ31 magnesium alloy tube manufactured by composite forming technology including extruded-shear and bending based on finite element numerical simulation and experiments

Hongjun Hu[1] · **Xing Hong**[1] · **Ye Tian**[1] · **Dingfei Zhang**[2]

Received: 9 November 2020 / Accepted: 4 May 2021 / Published online: 24 May 2021

Abstract
This paper presents a new forming technology for manufacturing the AZ31 magnesium alloy thin-wall tube. The direct extrusion process and continuous shearing-bending process are combined to produce thin-wall magnesium tube, abbreviated as "TESB" (tube extrusion-shearing-bending). The process has been studied based on the combination of experiments and numerical simulations, and the influences of temperatures, extrusion stresses, and friction factors on the forming process have been studied by Deform-3D simulation. And the mechanical properties and the grain size of the formed product have been tested. TESB technology has been proved to refine the grains of magnesium alloy tube effectively, and the mechanical property of the product can be improved. The better experimental extrusion conditions were also obtained by simulation, and the properties of the products under the condition of lubrication were better when the temperature was 400°C. Three-dimensional finite element modeling is used to investigate the plastic deformation behaviors of wrought magnesium alloy during TESB process. Numerical results indicate TES could increase the cumulative strains effectively by direct extrusion and additional shearings. Experiments show that microstructures of magnesium alloy fabricated by TESB process can be refined to 50% of the original grain size with more uniform distribution. TES process could improve hardness of magnesium alloy obviously by comparing with which fabricated by direct extrusion.

Keywords AZ31 magnesium alloy · Extrusion · Shearing · Tube · Finite element method · Microstructure · Experiment and simulation · Grain refinement

1 Introduction

The quality of the magnesium element is about 2.4% of the total mass of the earth's crust. In addition, magnesium is also distributed in seawater, salt lakes, and brine widely, such as Qinghai Salt Lake, where the reserves of magnesium chloride are as high as 8 billion tons, which exist in various forms, and magnesium alloys are inexhaustible metal materials [1–3]. Magnesium alloy, as a "green engineering material in the 21st century,", has high specific strength and specific stiffness, good dimensional stability, thermal conductivity, and strong vibration resistance; can withstand large impact load; and has excellent casting, machining performance, and easy recycling. These characteristics make it occupy a place in the aerospace field and can be used as aircraft, missiles, spacecrafts, satellites, etc. With the development of science and technology, the development of aerospace field is more and more inseparable from the participation of magnesium alloy [4].

In recent years, magnesium alloys are used in transportation, communication, electronics, and aerospace industries extensively. However, these alloys are difficult to be deformed at room temperature due to its hexagonal lattice structure with limited numbers of separate slip systems [5]. Although more than 90% of the magnesium alloy products are made by casting currently, large-scale production of wrought magnesium alloy products may be the future development direction. As comparing with magnesium alloy productions by casting process, the plastic deformation process can produce a variety of plates, rods, tubes, profiles, and forging products, and their strength, ductility and mechanical properties are higher than those made by casting.

As one of the key forming process, extrusion process is realized by plastic deformation under the action of three direction

✉ Hongjun Hu
hhj@cqut.edu.cn

1 Materials Science and Engineering College, Chongqing University of Technology, Chongqing 400050, China

2 National Engineering Research Center for Magnesium Alloys, Chongqing 400044, China

compression stresses. Therefore, extrusion process is suitable for the formation of low ductile materials, and which makes extrusion method an important method to produce deformed magnesium alloy products. However, the thermomechanical response of magnesium alloys affected by extrusion conditions is very complex. The experimental results show that the flow stresses and strain rates are not easy to be measured. In this case, finite element (FE) simulation can play a unique role in understanding the thermal-mechanical interaction in extruded materials [6]. The finite element simulation of extrusion process for magnesium alloy are reported. For example, it is assumed that the Mg-Zn-Zr alloy is thermoplastic and the temperature limit is defined by the FE for precision reverse extrusion. A two-dimensional finite element method is used to determine the size and capability of a press for extruding a magnesium-aluminum-zinc alloy in a temperature range [7]. In addition, the behavior of the AZ31 alloy in the extrusion forming process is predicted by the real-rigid plastic material model, and the heat exchange between the workpiece and the extrusion die is included [2].The variation of the grain size of the cross-section of the extruded sheet is explained by the stress and strain distribution. Other work makes use of iron to construct the limit view of the extrusion of the billet from the AZ31 billet into the rod [8].

In recent years, some new manufacturing processes and technologies have been used to process new magnesium alloy materials, such as die casting and semi-solid forming technology [3]. Large nanostructured materials treated by (SPD) with severe plastic deformation, such as equal channel angular extrusion (ECAE), have also attracted more and more attention from experts in the field of material science. (ECAE) process was invented in the early 1980s, but its development is not as much as people expected, and it is still limited to laboratory scale experiments [9–11].

In this paper, the direct extrusion process and continuous shearing-bending process are combined to produce thin-wall magnesium tube, abbreviated as "TESB" (tube extrusion shear-bending) in this paper. In order to illustrate the potential application of TESB process in industry, a complex extrusion die has been designed. The microstructure analysis and hardness testings of the tube fabricated by TESB process have been carried out. In this study, DEFORM^{TM}-3D finite element software is used to simulate the evolution of extrusion force, effective stress, and strain in TESB process.

2 Experimental and results

2.1 Experimental setup

Figure 1 illustrates the TESB process which combines direct extrusion with consecutive shearing process to fabricate fine grained AZ31 Mg alloy tube for the first time. In this process, the punch pushes the billets into the extrusion die. In the whole experiment, one time direction extrusion and two time shearings and one time bending deformation occurred. The extrusion tooling consists of die, container, and ram which are made of H13 hot-working tool steel. The die includes direction extrusion part with extrusion ratio 9. The used tooling and the press are shown in Fig. 2 a and b is the tube prepared by TESB process.

2.2 Microstructural analysis

The tube manufactured by TESB process is shown in Fig. 2b. The longitudinal direction along extrusion direction is chosen as the examined position for microstructural analysis on the processed tube. The metallographic structure was observed by picric acid 5g, glacial acetic acid 5g, distilled water 10ml, and ethanol 100ml. The metallographic structure was observed on Leica DMI5000M metallographic microscope. In order to analyze the microstructure evolution of AZ31 magnesium alloy during extrusion deformation and study the grain refinement mechanism of AZ31 magnesium alloy during TESB deformation, the four typical deformation of extruded products are sampled and analyzed; as shown in Fig. 3, the Fig. 3b is the primary shear zone, the Fig. 3c is the primary shear zone, and

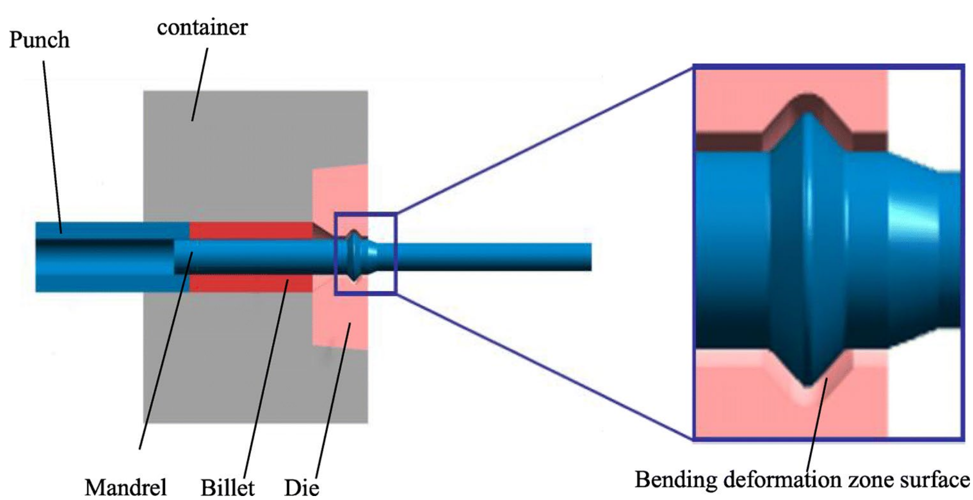

Fig. 1 Schematic of TESB process

Fig. 2 TESB equipment (**a**) and extruded tube (**b**)

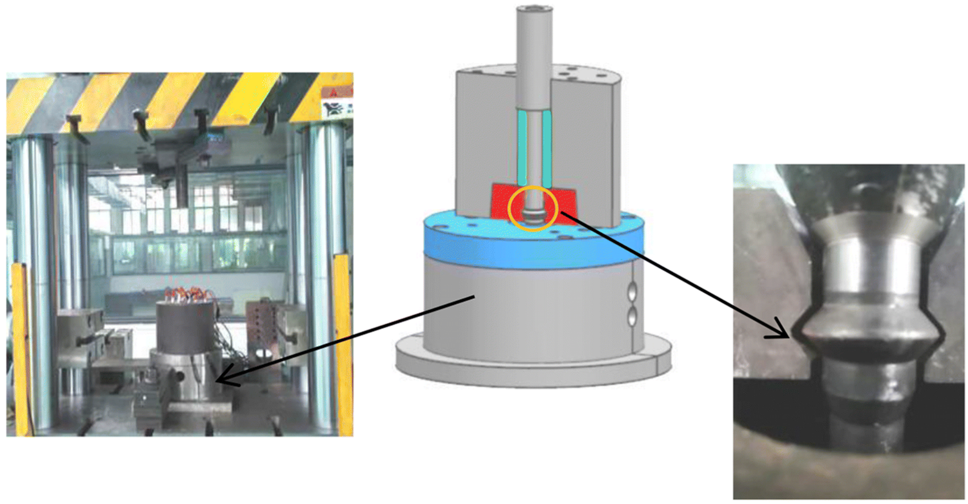

(a)

(b)

the Fig. 3d is the formed tube. The forming of the tube finally experienced two shear actions and one bending action. In Fig. 3a, the original grains of the as-cast AZ31 magnesium alloy billet is coarse and the average grain size is 82 μm.

From the metallographic diagram of Fig. 3c, it can be seen that the proportion of fine and recrystallized round grains increase obviously, which is due to the high deformation temperature, and with the increase of deformation degree, the distortion energy stored in the grains increase sharply and cannot be released in a short period of time, which increases the number of nucleation of recrystallized grains and further occurs dynamic recrystallization. Although many grains are already significantly refined after the process, the grain structure is more homogeneous than as-received, with very fine grains of 4–6μm as well as few coarse grains of greater than 25μm, and average grain size is 12μm.

The grains are subjected to strong triaxial stress, the dislocation density inside the grains increases sharply, and the lattice distortion intensifies. Although the grains in the Fig. 3d are no longer affected by stress after passing through the shear zone, the recrystallizing can continue, such as Fig. 3d. The diagram shows that the average grain size is reduced to 13.4μm from a large number of wafer grains below 10μm.

To sum up, a series of continuous deep shear deformation was introduced when AZ31 magnesium alloy thin-wall tube was extruded by TESB process. Only once extrusion can make the grain refinement effect of as-cast tube billet obvious, and the tube with uniform grain size is obtained

2.3 Microhardness test

The hardness is the mechanical property index used to measure the soft and soft degree of the material and the elastic-plastic and deformation characteristics of the reaction material. The extrusion and deformation process of the TESB of the AZ31 magnesium alloy tube blank includes the process of common extrusion, shearing, bending and the like, and the work hardening and dynamic recrystallization caused by the new pipe forming process have an important influence on the hardness of the material. Figure 4 shows the hardness distribution of the longitudinal section of each process in the process of extrusion and forming of the TESB at different temperatures. The numerical error range is about 5HV. As can be seen from the figure, during the whole TESB extrusion forming process, the hardness of the tube blank is decreased after the first increase, and the maximum hardness is

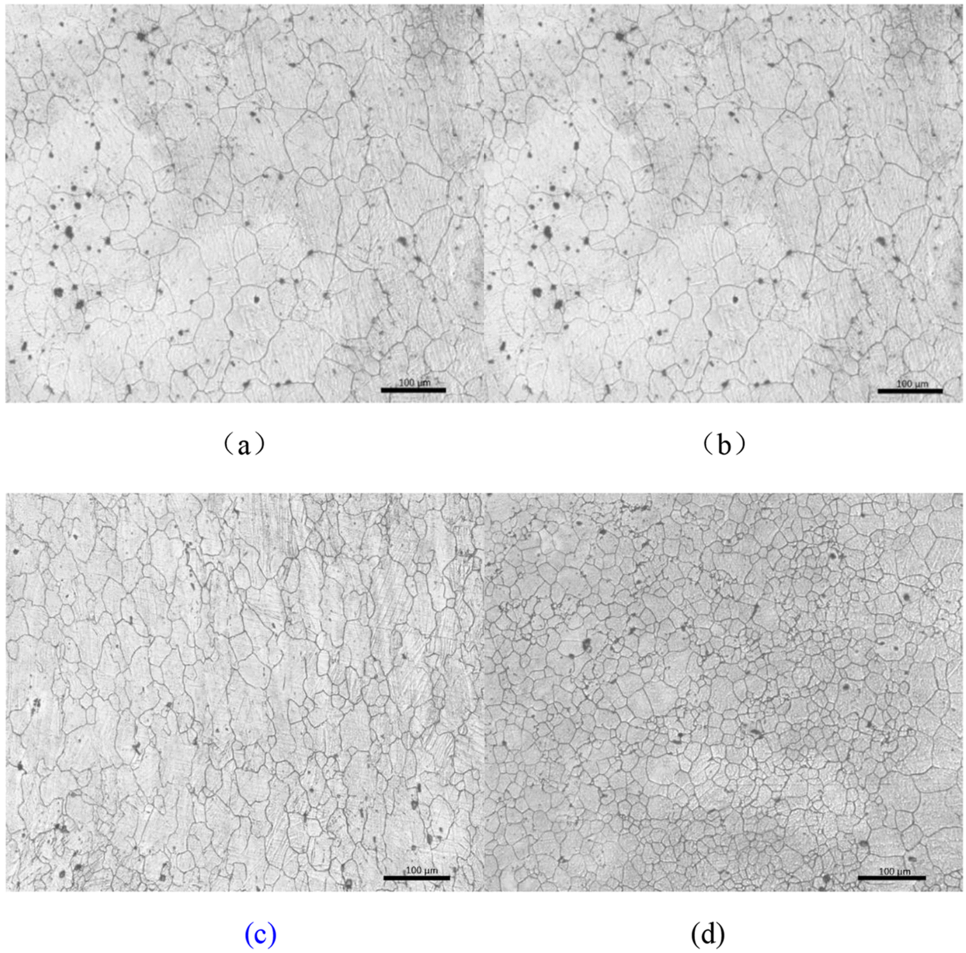

Fig. 3 The metallographic structure of the TESB extruded AZ31 magnesium alloy tube blank at different positions. **a** Common crush zone. **b** Primary shear zone. **c** Bending zone. **d** Shaped tube

72HV, 78HV, and 83HV, respectively. In that process of the early deformation, the deformation amount is gradually accumulated, the work hardening is serious, and the later-stage shaping stage, due to the friction action and the plastic deformation work, the temperature of the tube blank is high, the deformation energy storage is high, the dynamic recrystallization is fully carried out, the final grain generation is abnormal, and the crystal grain is reduced, and therefore the hardness is reduced. The higher the temperature, the lower the hardness value for each process location, which is due to the higher the temperature, the stronger the dislocation movement ability, and the lower dislocation entanglement, resulting in a decrease in hardness, and the final hardness of the formed pipe is 66 HV, 74 HV, and 79 HV, respectively.

3 FE model and results

3.1 FE model

DEFORM^{TM}-3D finite element software is used for modeling purpose [10, 12, 13]. The present study adopts the following assumptions: (1) both the container and the die are rigid bodies, (2) the extrusion billet is a rigid-plastic material, and (3) the friction factors between the extrusion billet and the ram, container, and die are constant following the generalized Coulomb's law [14, 15]. The material for simulation and experiment is commercial AZ31B (Mg-3%Al-1%Zn, wt) magnesium alloy, the composition of which is shown in Table 1.

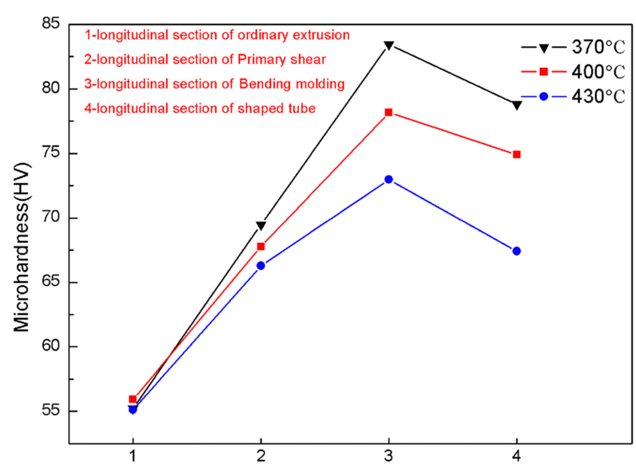

Fig. 4 Hardness distribution of longitudinal section of tube blank during TESB extrusion of AZ31 magnesium alloy

Table 1 The main element mass fraction of AZ 31 magnesium alloy (c%)

	Element			
	Al	Zn	Mn	Mg
Mass fraction %	2.5~3	0.7~1.3	>0.20	bal

Many parameters are involved in the process of extrusion, mold structure, and experimental conditions parameters such as extrusion temperature, extrusion speed, lubrication, or not. Each parameter has the influence to the extrusion process as well as the extrusion product. TESB process has the characteristics of ordinary extrusion; its mold structure is more complex. Therefore, the finite element simulation experimental parameters as shown in Table 2 are set (It mainly includes the billet size, extrusion ratio, minimum size of grid, etc., among the minimum grid size is determined by the minimum size of the die. In this experiment, minimum grid size is 1/3 of billet mesh size.) and the influence law of extrusion parameters on TESB process is studied by simulating extrusion pressure, metal flow, and temperature distribution under different parameter conditions.

In order to study the variation of real stress and strain with process parameters, the stress-strain curve is shown in Fig. 5. According to the curve regular in the figure, it can be found that at the same extrusion temperature, the stress of the material increases first and decreases with the increase of strain, subsequently. When the strain is the same, the stress of the material decreases with the increase of temperature.

3.2 FE results

3.2.1 Temperature field change

In order to study the temperature distribution of each part of the billet in the process of TESB deformation, the axial section of the billet is analyzed, as shown in the Fig. 6; when the initial extrusion temperature is 400 °C, the temperature distribution of the billet in the extrusion process is shown. During ordinary extrusion, the temperature in the undeformed area of the upper part of the billet does not change much. As shown in Fig. 6 (a, b), the temperature in the lower deformation zone of the billet increases obviously because at the beginning of plastic deformation, the heat of plastic deformation work transformation increases the temperature of the deformed area, and the billet passes through the ordinary extrusion zone, the diameter expansion shear zone, the bending zone, and the shrinkage shear zone in turn under the action of the extrusion rod, as shown in Fig. 6 (b). As shown by (c), (d), (e), the billet enters the stable deformation stage after the reduced diameter shear zone, and the extrusion load changes little at this stage. It is not difficult to see from the figure (e) that the shear deformation zone is the region with the highest temperature of the whole billet. The heat that causes the billet temperature to rise comes partly from its own plastic deformation work and partly from the friction between the billet and the die [16, 17]. Most of the plastic deformation work produced by the deformation of the billet increases the surrounding temperature in the form of heat,

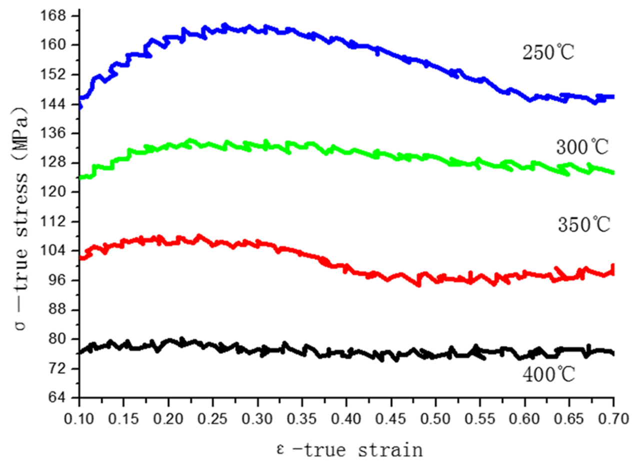

Fig. 5 Real stress-strain curve of AZ31 magnesium alloy

Table 2 Experimental parameters used in numerical simulation

Billet length(mm)	55
Billet outer diameter	39.6
Internal diameter of billet	20.4
Extrusion cylinder diameter	40
extrusion ratio	9.33
Thermal conductivity between billet and die(N/°C. S. mm^2)	11
Total number of grid elements	32000
Minimum size of grid	1.27
Relative penetration depth	0.7
Grid density type	opposite
Simulation type	Lagrangian incremental
Solver	Conjugate gradient with direct iteration

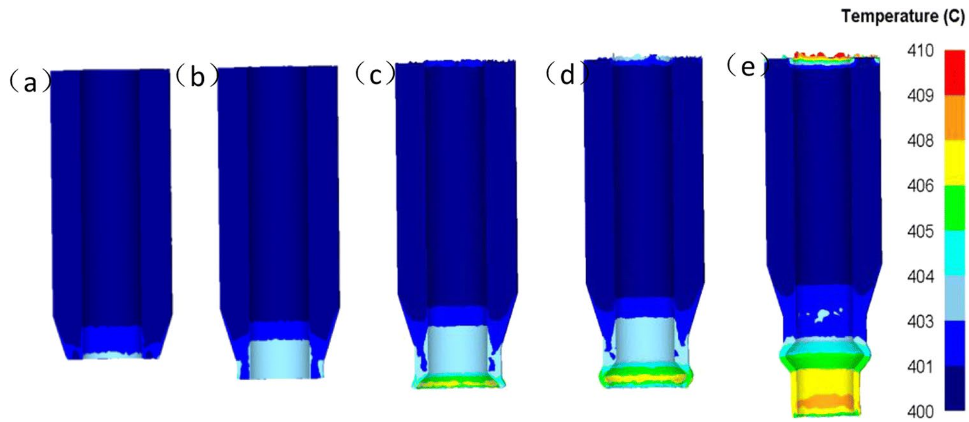

Fig. 6 The distribution of temperature field in different stages during the extrusion process

and very few of them remain in the interior of the billet in the form of crystal defects. On the whole, the temperature distribution in the deformation area of the billet is uniform, which is about 10 °C higher than the initial deformation temperature.

The shear deformation zone is always at high temperature in the whole extrusion process, which is also the key to determine the quality of the final extrusion pipe, which directly affects the microstructure and mechanical properties of the parts, and the large stress in the shear deformation zone, coupled with the sharp change of temperature, will also affect the dimensional accuracy of the die and then affect the size and shape of the extruded tube.

3.2.2 Effect of friction factor on equivalent effect stress

The change of friction factor will inevitably lead to the change of deformation load. Figure 7 shows the equivalent stress distribution in TESB extrusion process under different friction conditions. As shown in the figure, the shear deformation zone is the concentrated area of equivalent stress distribution. With the increase of friction factor, the blocking effect of die on billet flow increases, which leads to the increase of equivalent stress in shear deformation area. The overall analysis shows that the equivalent stress distribution of the billet is also changed due to the change of the contact conditions between the billet and the die [18]. Properly increasing the friction factor can make the equivalent stress distribution in the shear deformation region more uniform, which is similar to the back pressure applied to the deformed billet in the actual production process.

3.2.3 Effect of different temperatures on equivalent stress

Figure 8 shows the equivalent stress cloud diagram at extrusion speed of 10 mm/s and initial extrusion temperature of 370 °C, 400 °C, and 430 °C, respectively. It can be seen from the diagram that the equivalent force value in the shear deformation region is higher, and the maximum equivalent force value corresponding to the shear zone is different when the initial extrusion temperature is different. With the increase of deformation temperature, the

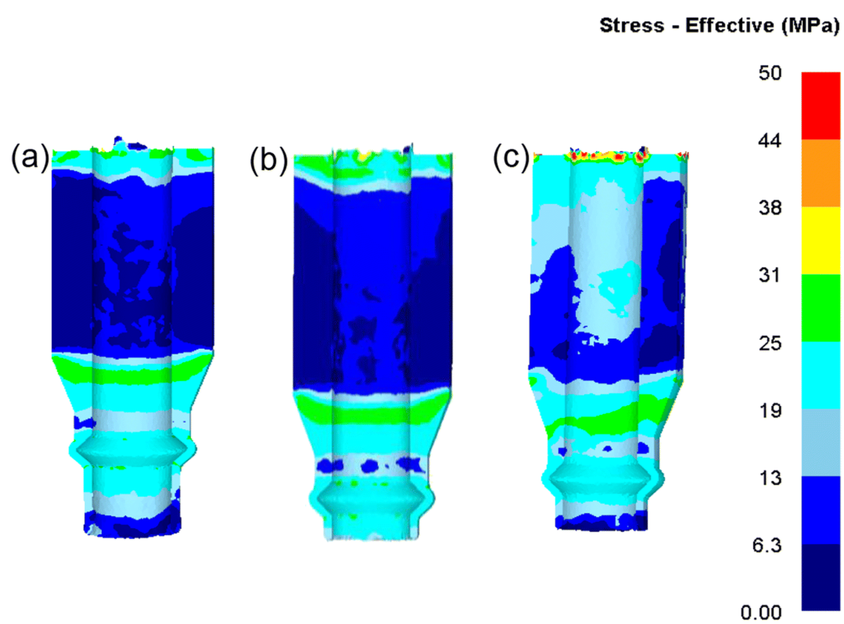

Fig. 7 Equivalent stress distribution of TESB extrusion of AZ31 magnesium alloy tube billet with the same friction factor. **a** 0.1. **b** 0.2. **c** 0.4

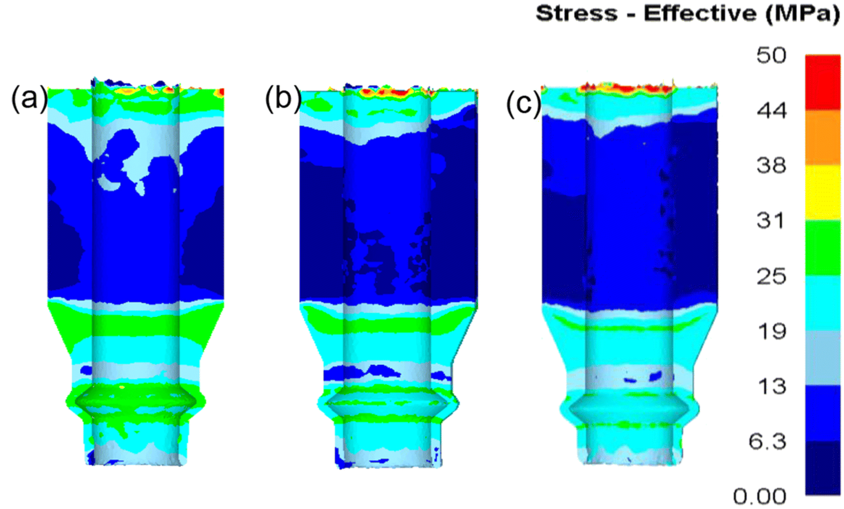

Fig. 8 Equivalent stress distribution of axial section of AZ31 magnesium alloy tube billet with different deformation temperatures. **a** 370°C. **b** 400°C. **c** 430°C

maximum equivalent stress in the shear zone decreases, and the uniformity of the equivalent stress distribution increases with the increase of the deformation temperature. In the process of plastic deformation of magnesium alloy billet, reasonable selection of deformation temperature is beneficial to prolong the life of die and improve the surface quality of the product [19, 20].

4 Conclusion

The bending process is added to the forming of magnesium alloy tube, which has obvious effect on the grain refinement of magnesium alloy tube. The grain size of magnesium alloy tube after bending process is about 1/7 of which prepared by direct extrusion. The grain size fabricated by direct extrusion is about 80μm and after bending process the grain size is about 13.4μ m.

Through the combination of finite element model and experiment, the high temperature region in the experimental process is mainly distributed in the deformation zone, and different friction factors will affect the stress and strain in the billet, and it is usually easier to obtain the pipe under the smaller friction factor. The effect of different temperature on stress distribution is that the higher the temperature, the smaller the stress distribution in the billet, but at the same time, too high temperature will lead to the coarse grain size and decrease the mechanical properties of the finished product. Therefore, the appropriate experimental parameters are very important for bending molding process.

Author contribution • Hongjun Hu is the corresponding author of this paper who wrote the paper.

- Xing Hong did the experiments
- Ye Tian did the examples in this paper.
- Dingfei Zhang researched the microstructures analysis in this paper.

Funding This work was supported by the National Science Foundation of China (52071042, 51771038, and 51571040); Chongqing Talent Plan (CQYC202003047); Chongqing Natural Science Foundation Project of cstc2018jcyjAX0249, cstc2018jcyjAX0653, and cstc2016jcyjA0434; Scientific and Technological Research Program of Chongqing Municipal Education Commission (KJ1600924); and Science and Technology Planning in Banan District of Chongqing City (No.0109184334).

I confirm that I have mentioned all organizations that funded my research in the Acknowledgements section of my submission, including grant numbers where appropriate.

Data availability The raw/processed data required to reproduce these findings cannot be shared at this time as the data also forms part of an ongoing study.

Declarations

Ethical approval No animals have been used in any experiments.

Consent to participate There are no human who have been used in any experiments.

Consent for publication The author confirms:

- That the work described has not been published before (except in the form of an abstract or as part of a published lecture, review, or thesis)
- That it is not under consideration for publication elsewhere
- That its publication has been approved by all co-authors, if any
- That its publication has been approved (tacitly or explicitly) by the responsible authorities at the institution where the work is carried out.

The author agrees to publication in the Journal indicated below and also to publication of the article in English by Springer in Springer's corresponding English-language journal.

The copyright to the English-language article is transferred to Springer effective if and when the article is accepted for publication. The author warrants that his/her contribution is original and that he/she has full power to make this grant. The author signs for and accepts responsibility for releasing this material on behalf of any and all co-authors. The copyright transfer covers the exclusive right to reproduce and distribute the article, including reprints, translations, photographic reproductions, microform, electronic form (offline, online), or any other reproductions of similar nature.
After submission of the agreement signed by the corresponding author, changes of authorship or in the order of the authors listed will not be accepted by Springer.

Competing interests The authors declare no competing interests.

References

1. Basavaraj VP, Chakkingal U, Kumar TSP (2009) Study of channel angle influence on material flow and strain inhomogeneity in equal channel angular pressing using 3d finite element simulation. J Mater Process Technol 209:89–95
2. Figueiredo RB, Cetlin PR, Langdon TG (2007) The processing of difficult-to-work alloys by ecap with an emphasis on magnesium alloys. Acta Mater 55:4769–4779
3. Faraji G, Yavari P, Aghdamifar S, Mashhadi MM (2014) Mechanical and microstructural properties of ultra-fine grained AZ91 magnesium alloy tubes processed via multi pass tubular channel angular pressing (TCAP). J Mater Sci Technol 30:134–138
4. Abdolvand H, Faraji G, Shahbazi Karami J, Baniasadi M (2017) Microstructure and mechanical properties of fine-grained thin-walled az91 tubes processed by a novel combined spd process. Bull Mater Sci 40(7):1471–1479
5. Fata, A., Faraji, G., Mashhadi, M. M., & Abdolvand, H.. (2016). Evaluation of hot tensile behavior of fine-grained mg–9al–1zn alloy tube processed by severe plastic deformation. Transactions of the Indian Institute of Metals, 1-8
6. Zhang D, Hu H, Pan F, Yang M, Zhang J (2010) Numerical and physical simulation of new SPD method combining extrusion and equal channel angular pressing for AZ31 magnesium alloy. Trans Nonferrous Metals Soc China 20:478–483
7. Liu G, Zhou J, Duszczyk J (2007) Finite element simulation of magnesium extrusion to manufacture a cross-shaped profile. J Manuf Sci Eng 129:607–614
8. Hu HJ, Huang WJ (2013) Effects of turning speed on high-speed turning by ultrafine-grained ceramic tool based on 3D finite element method and experiments. Int J Adv Manuf Technol 67:907–915
9. Zhao ZD, Chen Q, Chao HY, Huang SH (2010) Microstructural evolution and tensile mechanical properties of thixoforged ZK60-Y magnesium alloys produced by two different routes. Mater Des 31:1906–1916
10. Chen Q, Zhao ZD, Chen G, Wang B (2015) Effect of accumulative plastic deformation on generation of spheroidal structure, thixoformability and mechanical properties of large-size AM60 magnesium alloy. Journal of Alloys & Compounds 632:190–200
11. Chen Q, Yuan BG, Lin J, Xia XS, Zhao ZD, Shu DY (2014) Comparisons of microstructure,thixoformability and mechanical properties of high performance wrought magnesium alloys reheated from the as-cast and extruded states. Journal of Alloys & Compounds 584:63–75
12. Chen Q, Zhao ZD, Zhao ZX, Hu CK, Shu DY (2011) Microstructure development and thixoextrusion of magnesium alloy prepared by repetitive upsetting-extrusion. Journal of Alloys & Compounds 509:7303–7315
13. Chen Q, Chen G, Han LN, Hu N, Han F, Zhao ZD, Xia XS, Wan YY (2015) Microstructure evolution of sicp/ZM6 (Mg-Nd-Zn) magnesium matrix composite in the semi-solid state. Journal of Alloys & Compounds 656:67–76
14. Hu H, Zhai Z, Li Y, Wang H, Dai J (2015) Researches on physical field evolution of micro-cutting of steel H13 by micron scale ceramic cutter based on finite element modeling. Int J Adv Manuf Technol 78(9-12):1407–1414
15. Hu H-J, Huang W-J (2013) Studies on wears of ultrafine-grained ceramic tool and common ceramic tool during hard turning using Archard wear model. Int J Adv Manuf Technol 69(1-4):31–39
16. Hu H-J, Wang H, Zhai Z-Y, Li Y-Y, Fan J-Z, Zhongwen OU (2014) The influences of shear deformation on the evolutions of the extrusion shear for magnesium alloy. Int J Adv Manuf Technol 174(1-4):423–432
17. Hu H-J, Wang H, Zhai Z-Y, Li Y-Y, Fan J-Z, Ou Z-W (2014) Effects of channel angles on extrusion-shear for AZ31 magnesium alloy: modeling and experiments. Int J Adv Manuf Technol 76(9-12):1621–1630
18. Mofid MA, Abdollah-zadeh A, Gür CH (2014) Investigating the formation of intermetallic compounds during friction stir welding of magnesium alloy to aluminum alloy in air and under liquid nitrogen. Int J Adv Manuf Technol 71(5-8):1493–1499
19. Feng F, Huang S, Hu J, Meng Z, Lei Y (2013) Analysis of the bulging process of an AZ31B magnesium alloy sheet with a uniform pressure coil. Int J Adv Manuf Technol 69(5-8):1537–1545
20. Rajakumar S, Razalrose A, Balasubramanian V (2013) Friction stir welding of AZ61A magnesium alloy. Int J Adv Manuf Technol 68(1-4):277–292